Am. J. Trop. Med. Hyg., 92(5), 2015, pp. 887–897
doi:10.4269/ajtmh.14-0497

Trypanosoma cruzi Calreticulin Topographical Variations in Parasites Infecting Murine Macrophages

Andrea González, Carolina Valck, Gittith Sánchez, Steffen Härtel, Jorge Mansilla, Galia Ramírez, María Soledad Fernández, José Luis Arias, Norbel Galanti,* and Arturo Ferreira*

Programa Disciplinario de Inmunología, Programa de Genética Humana, Programa de Biología Celular y Molecular, Instituto de Ciencias Biomédicas; Laboratorio de Análisis de Imágenes Científicas (SCIAN), Instituto de Neurociencias Biomédicas, Facultad de Medicina; Departamento de Medicina Preventiva Animal, Departamento de Ciencias Biológicas Animales, Facultad de Ciencias Veterinarias y Pecuarias, Universidad de Chile, Chile

Abstract. *Trypanosoma cruzi* calreticulin (TcCRT), a 47-kDa chaperone, translocates from the endoplasmic reticulum to the area of flagellum emergence. There, it binds to complement components C1 and mannan-binding lectin (MBL), thus acting as a main virulence factor, and inhibits the classical and lectin pathways. The localization and functions of TcCRT, once the parasite is *inside* the host cell, are unknown. In parasites infecting murine macrophages, polyclonal anti-TcCRT antibodies detected TcCRT mainly in the parasite nucleus and kinetoplast. However, with a monoclonal antibody (E2G7), the resolution and specificity of the label markedly improved, and TcCRT was detected mainly in the parasite kinetoplast. Gold particles, bound to the respective antibodies, were used as probes in electron microscopy. This organelle may represent a stopover and accumulation site for TcCRT, previous its translocation to the area of flagellum emergence. Finally, early during *T. cruzi* infection and by unknown mechanisms, an important decrease in the number of MHC-I positive host cells was observed.

INTRODUCTION

American Trypanosomiasis (Chagas' disease) currently affects over 10 million people, and the infection now spreads worldwide.[1–3] Its etiological agent is *Trypanosoma cruzi*, a hemoflagellate protozoan parasite. The infective trypomastigote enters the insect vector when it feeds from an infected mammal host. In the stomach of the insect, trypomastigotes transform into non-infective epimastigotes, which replicate in the gut, adhere to intestinal cells, and transform into metacyclic trypomastigotes that are eliminated with feces.

These trypomastigotes infect vertebrate hosts, and once in the bloodstream, they penetrate host cells, through a parasitophorous vacuole (a host cell vacuole, occupied by the parasite). There, they transform into replicating amastigotes that differentiate into trypomastigotes that are released to the extracellular space and from there into the bloodstream, where they penetrate other cells, starting a new cycle.[4] The infective process begins when the flagellum emergence zone (a distal part of the trypomastigote, where the flagellum emerges in close proximity to the flagellum pocket), establishes the first contact with the host cell membrane. To maintain this cycle and consequently, its survival, the parasite uses multiple strategies to evade the host immune system. One of its main virulence factors is calreticulin (TcCRT),[5] a 47 kDa lectin chaperone, highly conserved among species, bearing an endoplasmic reticulum (ER)-retention signal KEDL on the carboxi-terminus domain,[6] similar to mammalian CRT.[7,8] The TcCRT is also present in other organelles in free parasites, including Golgi, cytoplasm, nucleus, and kinetoplast.[9]

In mammals, calreticulin (CRT) has major roles in key cell functions, such as protein folding regulation (i.e., MHC-I), calcium storage and signaling, transcription regulation, cell adhesion, and autoimmunity, among others. Its vital importance is highlighted by the fact that *CRT* –/– KO mice die *in utero* 14 days post-fertilization.[10] The TcCRT is translocated from the ER to the flagellum emergence zone[11] where through its central S domain, interacts with C1, thus inhibiting the early stages of the complement classical pathway.[11,12] The TcCRT, by virtue of its capacity to bind and inactivate complement C1 acts as a main virulence factor. Inactive C1 remains bound to the parasite (acting as an "eat me" signal), thus mediating its interaction with host cell CRT.[5,13] The lectin complement pathway is also inhibited because TcCRT interacts with the mannan-binding lectin (MBL) and ficolins.[14] Through a different domain, located in the amino terminal sequences, extracellular TcCRT interacts with endothelial cells, most likely through a collagen-like Scavenger-Receptor class A, because this interaction is inhibited by fucoidan, an homopolymer of sulfated L-fucose,[15] (Abello and others, 2014, unpublished). The interactions of TcCRT with endotheliocytes mediate antiangiogenic and antitumor effects.[15–17]

Monoallelic *TcCRT* KO parasites, the wild-type, and a transgenic variant (with an extra *TcCRT* gene copy), display increasing survival capacity in the presence of human complement, and enhanced *in vivo* infectivity (*TcCRT* homozygous KO parasites are not viable).[18,19]

Parasite TcCRT location *once the parasite is inside the mammal cell* has not been reported, as well as its functional roles in those new locations. Herein, we describe strategies to detect TcCRT in those parasite forms infecting a murine macrophage cell line, as compared with free trypomastigotes and non-infective epimastigotes. We propose that the kinetoplast may represent a necessary stopover, previous to the translocation of TcCRT to the area of flagellum emergence, in response to the new environmental conditions that the parasite meets inside the host cell.

MATERIALS AND METHODS

Recombinant TcCRT (rTcCRT). The rTcCRT was generated as described.[20] In brief, *TcCRT* without its leader and its KEDL ER retention signal, was amplified by polymerase

*Address correspondence to Arturo Ferreira or Norbel Galanti, Independencia 1027, Independencia, Santiago, Chile. E-mails: aferreir@med.uchile.cl or ngalanti@med.uchile.cl

chain reaction (PCR) and ligated to a pET-28b(+) vector. The rTcCRT was expressed from *Escherichia coli* BL21 (DE3)pLysS, transformed with the pET-28b (+)/*TcCRT* plasmid, and the recombinant molecule was purified by affinity chromatography.

Polyclonal antibodies. A rabbit polyclonal antiserum was generated against rTcCRT.[6,21] Previous to the immunization, a preimmune serum was obtained. By serial dilutions, the immune serum had a titer of 10^{-6}, when tested against solid-phase bound rTcCRT. These antibodies did cross-react with murine calreticulin (MmCRT), when tested in immuno-western blot (IWB), up to dilution of 1/8,000 v/v, against a whole cell extract of the murine macrophage cell line RAW 264.7 (data not shown). When tested in transmission electron microscopy (TEM), minimal cross-reactivity against MmCRT was observed in dilution 1/32,000 v/v (Supplemental Figure 1). This dilution was chosen for TcCRT TEM detections.

Monoclonal antibody. A monoclonal IgG1 anti-TcCRT antibody E2G7 was generated against native purified TcCRT,[22] as described, using standard protocols.[23] The E2G7 purification from mouse ascites was performed by affinity chromatography. The E2G7 specificity was corroborated in an indirect enzyme-linked immunosorbent assay (ELISA) (Supplemental Figure 2).

Cell culture. The 5×10^6 murine macrophages (RAW 264.7 cells) were infected with 5×10^7 trypomastigotes (Dm28c strain). Cell culture was performed in RPMI medium supplemented with 10% v/v fetal bovine serum (FBS), 1% v/v penicillin/streptomycin, and 1% v/v glutamine, at 37°C. Cells were harvested at 2, 4, and 6 h post infection (PI), and processed for TEM. As control, 5×10^6 non-infected macrophages were harvested simultaneously.

Parasites. *Trypanosoma cruzi* trypomastigotes (Dm28c strain) were maintained in RPMI medium supplemented with 10% v/v FBS, 1% v/v penicillin/streptomycin, and 1% v/v glutamine at 37°C. The 1.5×10^8 extracellular trypomastigotes were obtained from the supernatant of infected mammalian VERO cells[5] (isolated from kidney epithelial cells extracted from an African green monkey[24]) and processed for TEM. *Trypanosoma cruzi* epimastigotes (Dm28c strain) were cultured in 80 mL of Diamond Medium (Tryptose, Tryptone, and yeast extract, at 6.25 g/l each; 0.107 M NaCl, 0.03 M KH_2PO_4, 0.022 M K_2HPO_4, pH 7.2) supplemented with neonate bovine serum (NBS), penicillin/streptomycin, and hemin, at 27°C. The 1.5×10^8 epimastigotes were processed for TEM.

TEM. Infected and non-infected cells were harvested, washed twice with phosphate-buffered saline (PBS), fixed in glutaraldehyde 3% v/v in phosphate buffer (sodium phosphate 0.1 M, pH 7.3) overnight (o.n.) at 4°C, washed, and post-fixed with osmium tetroxide 1% v/v in phosphate buffer. Samples were rinsed and progressively dehydrated in 30% up to absolute ethanol, treated with acetone, and finally embedded in EPON resin 812 at 70°C. Ultrathin sections (700 A°), were placed on copper grids, stained with 5% w/v aqueous uranyl acetate, and 0.04% w/v lead citrate, and then observed in electron microscope (Zeiss EM-109, Jena, Germany), at 80 kV.

Immunocytochemistry. Performed similarly as described,[9] with some modifications in the inclusion process (in which the sample is embedded in a new resin, after impregnation, and allowing polymerization for 48 hrs minimum at high temperature). Basically, cells and parasites were fixed in 4% w/v paraformaldehyde plus 0.1% glutaraldehyde v/v in cacodylate buffer (pH 7.2) o.n. at 4°C. Free aldehyde groups were blocked with 50 mM ammonium chloride. Samples were rinsed and sequentially dehydrated in 30% up to absolute ethanol, at room temperature, and embedded in Poly Bed 812 resin at 60°C. Ultrathin sections of 700 A° were obtained, collected on nickel grids, and, after immunocytochemical procedures, were stained with 5% w/v aqueous uranyl acetate. Finally, samples were observed at 80 kV in a Zeiss EM-109 and in a Phillips-TECNAI 12 electron microscopes (Eindhoven, The Netherlands).

Immunocytochemical procedures for CRT detection. Nickel grids containing sections of 700 A° were floated, for 30 min at room temperature, in TRIS 0.02 M pH 7.2 containing 0.02% w/v sodium azide, 0.15 M sodium chloride, 0.1% w/v bovine serum albumin (BSA), and 0.05% v/v Triton X-100 (immunostain buffer). The sections were then incubated o.n. at 4°C with a primary antibody (Polyclonal anti-rTcCRT 1/32,000 v/v or monoclonal E2G7 1/100 v/v) diluted in immunostain buffer. After washing in immunostain buffer, sections were incubated for 2 h with a secondary antibody (Goat anti-rabbit IgG conjugated to 10 nm diameter colloidal gold, Sigma G7402 [St. Louis, MO], or goat anti-mouse IgG conjugated to 18 nm diameter colloidal gold, Abcam ab105289 [Cambridge, UK]), diluted 1/20 v/v in immunostain buffer, prior to centrifugation for 10 min at $2{,}000 \times g$. After washing, the sections were rinsed with deionized water. Controls include sections incubated with pre-immune serum, and isotype control (IgG1), performed in parallel, in the same conditions used with the primary antibody. Additionally, the sample was incubated o.n. with immunostain buffer, followed by incubation with the respective secondary antibody, as previously described.

Quantification of label density generated by polyclonal antibodies. Gold particles (GPs)/μm^2 in different compartments of the host cell were quantified using Image Analysis Routines (SCIAN-Soft, Santiago, Chile) based on interactive data language (IDL) 7.1 (ITT, Boulder, CO). For statistical analysis, the sub-cellular compartments of four different cells per condition were analyzed.

Quantification of TcCRT molecules in kinetoplast sections. Because 18 nm GPs are easily resolved, their numbers in kinetoplast sections, obtained from different parasite stages, were quantified by their direct observation on TEM photographs located under a transparent film. Each GP was counted out by labeling it on the transparent film, using a marker. Each photo was counted three times, and the average value of minimum five photos per condition was used for statistical analysis.

ELISA. To evaluate the E2G7 MoAb specificity, microtiter plates were sensitized with 100 µL of E2G7 or anti-HuCD45 (a leukocyte common antigen, isotype negative control) per well, 5 µg/mL, in carbonate buffer o.n. at 4°C. Non-reactive sites were blocked with PBS-BSA 5% w/v for 2 h at 37°C. Plates were washed four times with PBS-Tween 0.05% v/v, and then 100 µL of TcCRT 1.25 µg/mL was added per plate and incubated for 2 h at 37°C. The rHuCRT was used as the antigen control. After washing, a polyclonal anti-TcCRT antibody 1/5,000 v/v was incubated for 1.5 h at 37°C. A pre-immune serum was used as control. A secondary anti-rabbit-IgG conjugated to peroxidase 1/1,000 v/v was incubated for 1.5 h at 37°C, after washing with PBS-Tween 0.05% v/v. Finally, after a wash with PBS, 100 µL per well of ABTS-H_2O_2 30% v/v was added and the plates were read at 405 nm.

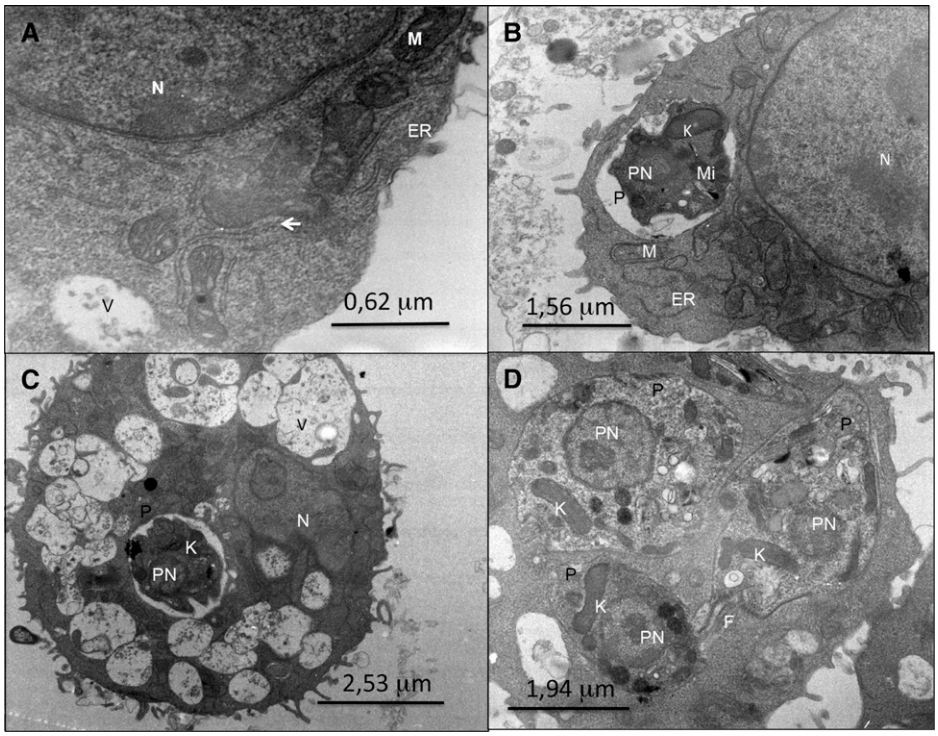

FIGURE 1. Host cell and parasite organelles are resolved by electron microscopy in infected macrophages. Electron microphotographs of infected and non-infected murine macrophages are shown (**A**) in a non-infected cell (30,000×), ribosomes are resolved (arrow). Parasite sections (P) are shown inside macrophages at different hours post-infection; (**B**) Inside a parasitophorous vacuole, at 2 h (20,000×); (**C**) at 4 h (7,000×), in a vacuolated host cell, and (**D**) at 6 h (12,000×), three parasite sections are observed free in the cytoplasm. In host cell: ER = endoplasmic reticulum; M = mitochondria; N = nucleus; V = vacuole. In parasites: P = parasite; K = kinetoplast; F = flagellum; Mi = mitochondrion; PN = parasite nucleus.

Detection of positive cells for MHC class I antigens by flow cytometry. The 5×10^5 RAW cells were infected for 2, 4, and 6 h with 5×10^6 trypomastigotes (Dm28c strain), each condition in triplicate. The 5×10^5 non-infected RAW 264.7 cells were used as control. Cells were washed twice in PBS 1× (380 g for 5 minutes each), placed on a V- bottom microtiter plate, incubated with 100 μL of MoAb anti-H2D^d, conjugated to fluorescein-isothiocyanate (FITC)

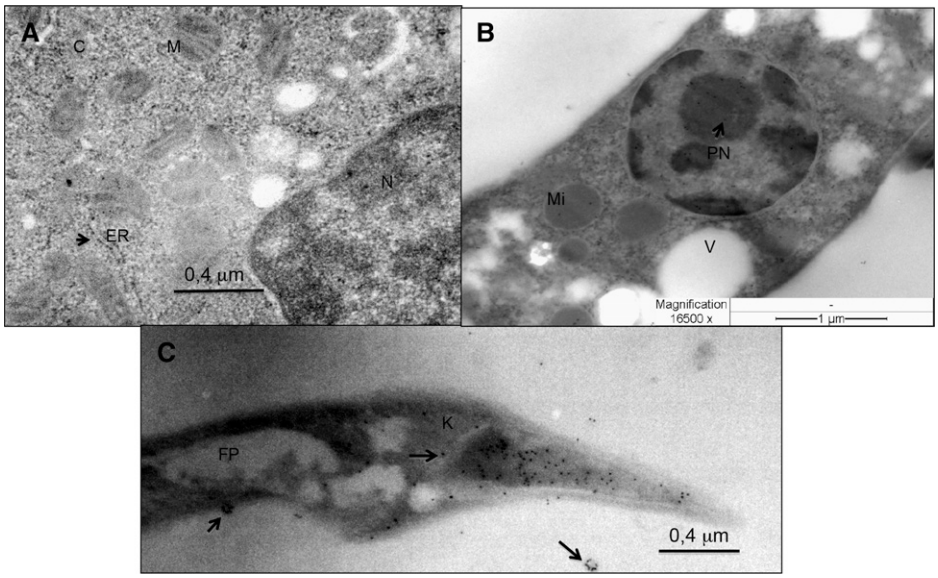

FIGURE 2. Calreticulin is detected in free parasites and in non-infected host cell organelles. Electron microphotographs of non-infected cell and free parasites are shown. Gold particles are observed in (**A**) a non-infected cell (30,000×), in the nucleus (N), cytoplasm (C), and the endoplasmic reticulum (ER). (**B**) A free epimastigote (16,500×), in the nucleus (N). (**C**) A free trypomastigote (30,000×), in the kinetoplast and the flagellum emergence zone, and in vesicle-like structures (arrows). In host cell: ER = endoplasmic reticulum; M = mitochondria; N = nucleus; C = cytoplasm. In parasites: K = kinetoplast; FP = flagellum pocket; V = vacuole; Mi = mitochondrion; PN = parasite nucleus. Arrows: positive signals.

(BD Bioscience, Cat. no. 553579, 1/50 v/v, East Rutherford, NJ), per well, 30 min. in darkness. Samples were washed twice with PBS 1×, fixed with p-formaldehyde 1%, 100 μL per well, 30 min at 4°C, washed, and stored at 4°C.

Flow cytometry data analysis. Data were obtained in a FACSCalibur-4 color flow cytometer (Becton Dickinson, East Rutherford, NJ, 2007), and were analyzed with the program FlowJo 8.7, Mackintosh version, Tree Star Incorporated (Ashland, OR).

Statistical analysis. The number of GPs, positive MHC-I cells, and indirect ELISA were statistically validated using one and/or two-way analysis of variance (ANOVA) tests. Both tests were performed with Graphpad Prism 5.0, Macintosh version, Software Mackiev, Graphpad software Inc. (La Jolla, CA).

RESULTS

As a proper topographic control, the murine macrophage cell line RAW 264.7, was infected with trypomastigotes (Dm28c strain), as described in Methods. Sections of infected and non-infected cells were processed for TEM. Resolution seems adequate because ribosomes can be observed in non-infected RAW cells (Figure 1A). At 2 and 4 h PI (Figure 1B and C, respectively), parasites can be observed inside the parasitophorous vacuole and, at 6 h PI, parasites are also found free in the host cell cytoplasm (Figure 1D). Multiple vacuoles are seen at 4 h PI (Figure 1C), as discussed below.

In immunocytochemistry, a representative set of results corresponding to infected and non-infected RAW 264.7 cells incubated with the anti-TcCRT PoAb is shown in Figures 2 and 3. In non-infected macrophages, some GPs can be observed, which could correspond to background reactivity with MmCRT. Some particles were observed in the nucleus, cytoplasm, and, as expected, in the ER (Figure 2A). In free epimastigotes, as expected,[9] the label was observed basically in the nucleus (Figure 2B). In agreement with previous results[9,11] in free trypomastigotes (Figure 2C), GPs were observed in the kinetoplast, and an apparent flow toward the flagellum emergence zone can be proposed. Furthermore, as expected,[9] particles are found in vesicles near (or emerging) from the trypomastigote. At 2 h PI, GPs were observed in the parasitophorous vacuole, and in the host cell cytoplasm. In the parasite, nucleus and kinetoplast are among the organelles where a high-density label can be observed. Some GPs

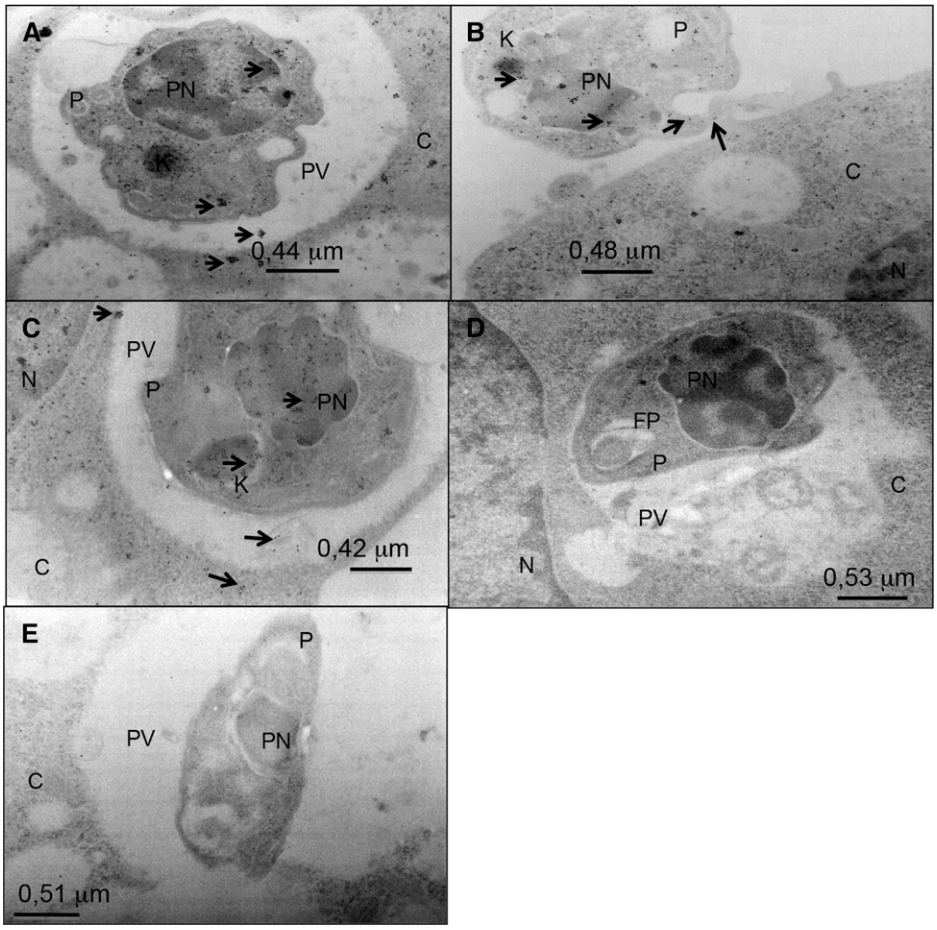

FIGURE 3. Calreticulin is detected in infected cells. After infection, gold particles were detected at (**A**) 2 h, in the parasite nucleus and kinetoplast, in the host cell cytoplasm, and in vesicle-like structures (arrows); (**B**) 4 h, in a parasite outside the host cell, in the parasite nucleus and kinetoplast, in the host cell nucleus and cytoplasm; (**C**) 6 h, in the parasite nucleus and kinetoplast, and in vesicle-like structure in the host cell cytoplasm (arrow); (**D** and **E**) 6 h, control samples. No gold particles were observed. (**A**–**C**) Anti-rTcCRT polyclonal serum, 1/32,000 v/v; (**D**) anti-rabbit IgG conjugated to colloidal gold (10 nm), 1/20 v/v; (**E**) pre-immune serum 1/32,000 v/v. In host cell: N = nucleus; C = cytoplasm; PV = parasitophorous vacuole. In parasites: P = parasite; K = kinetoplast; FP = flagellum pocket; V = vacuole; Mi = mitochondrion; PN = parasite nucleus. Arrows: positive signals. All samples are 30,000×.

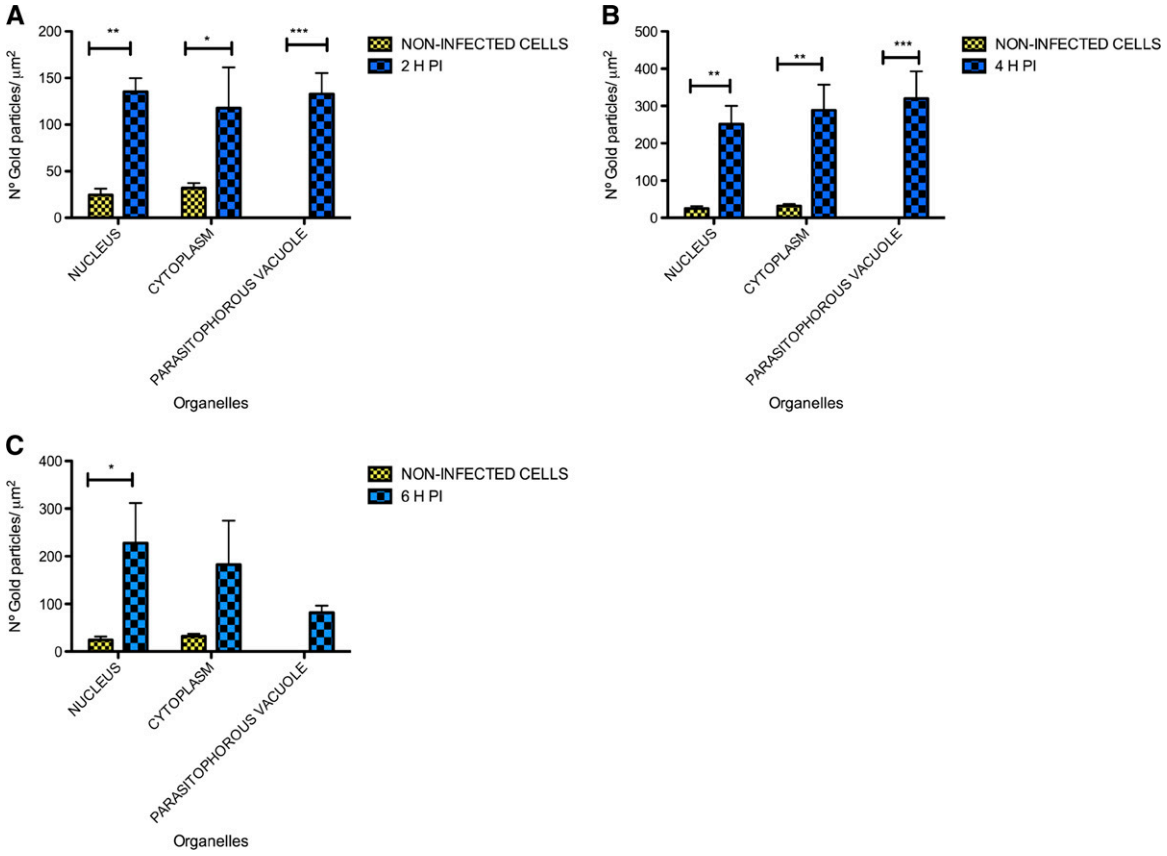

FIGURE 4. Calreticulin concentration detected with the polyclonal anti-rTcCRT antibodies is higher in infected cells. At 2 and 4 h PI, more gold particles are detected in the nucleus and cytoplasm (**A** and **B**). The average number of particles found in the parasitophorous vacuole is included for comparison purpose. (**C**) Gold particles detected in nucleus, at 6 h PI. (**A**–**C**) Two-way ANOVA * = $P < 0.05$ ** = $P < 0.01$ *** = $P < 0.001$. Bars: Standard deviations.

are also found in structures similar to those observed in free trypomastigotes, *inside* the parasitophorous vacuole (*outside* the parasite), in the borderline of the parasitophorous vacuole, and in the host cell cytoplasm (Figure 3A, arrows). At 4 h PI, a parasite was observed outside the host cell, probably before being phagocytosed. GPs were detected in several organelles in the parasite, but more condensed in the nucleus and kinetoplast. In the host cell, GPs are observed in the cytoplasm and nucleus (Figure 3B). At 6 h PI, GPs were observed in the parasitophorous vacuole. In the host cell, GPs were observed at the nucleus and cytoplasm (Figure 3C). As observed previously (Figure 2C and Figure 3A), there was a label concentration on structures similar to vesicles on the edge of the parasitophorous vacuole (arrowhead). These structures are consistent with those previously described.[9] No GPs were observed in 6 h PI samples incubated with just the secondary gold-labeled antibody (Figure 3D) or with pre-immune sera (Figure 3E).

GPs/μm^2, in different compartments of the host cell, were quantified as described in Methods. Non-infected cells showed a lower number of GPs in the analyzed cellular compartments, compared with 2 h PI ($P < 0.05$ in cytoplasm, $P < 0.01$ in nucleus, Figure 4A). A similar situation was observed when compared with 4 h PI ($P < 0.01$ in nucleus and cytoplasm, Figure 4B). The only variation between the two conditions was the label in the cytoplasm, which increases at 4 h PI. When non-infected cells were compared with cells at 6 h PI, the nucleus was the only organelle that presented significantly more GPs in the infected cells (Figure 4C). In the parasitophorous vacuole, the number of GPs decreases at 6, compared with 2 and 4 h PI.

The CRT is a key molecule on the MHC-I folding process.[25–28] An increase of CRT molecules was detected with the polyclonal anti-TcCRT antibodies in infected host cell cytoplasm (Figure 4). Therefore, we asked whether this CRT expression correlates with that of MHC class I molecules. By flow cytometry, surface MHC-I positive cells were identified as described in Methods, in non-infected and infected RAW 264.7 cells. Less MHC-I positive cells are detected at 2 and 4 h PI (Figure 5A and C) compared with non-infected cells. The 6 h PI sample is similar to the non-infected counterpart. The percentage of maximum fluorescence was similar in all samples studied (Figure 5B).

The TcCRT detection with a monoclonal antibody (E2G7), generated against the purified native protein, was performed as described in Methods. A representative set of results corresponding to infected and non-infected RAW 264.7 cells is shown in Figures 6 and 7. In free parasites (Figure 6A), GPs are observed almost exclusively in the kinetoplast. In non-infected RAW 264.7 murine macrophages (Figure 6B), some GPs are detected in the nuclear heterochromatin, and also in the cytoplasm, most likely as a non- specific background label. In free epimastigotes (Figure 6C) label is observed basically in the nucleus, although at a much

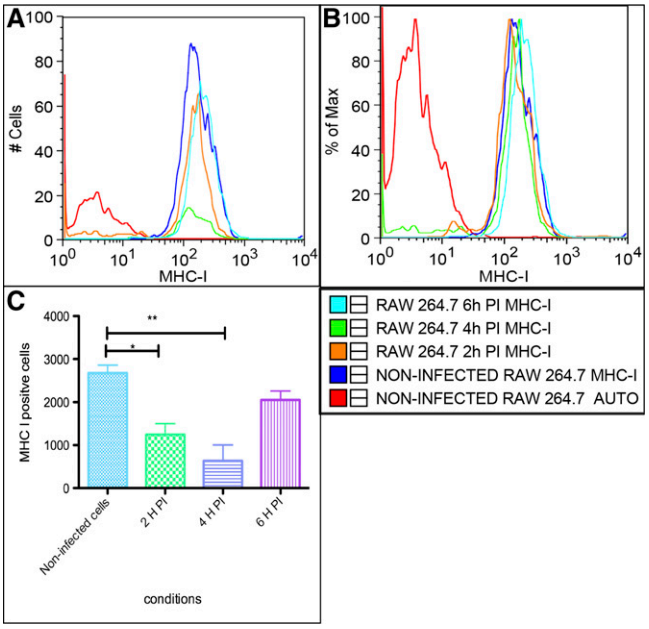

FIGURE 5. MHC-I positive cells decrease at 2 and 4, but not at 6 h PI, as detected by flow cytometry. Representative cytometry histograms are shown. (**A**) Number of MHC-I positive cells decrease at 2 and 4 h PI, whereas the 6 h PI sample remained similar to the non-infected counterpart. (**B**) Percentage of maximum fluorescence was similar in all samples analyzed, which is indicative of no variation of surface MHC-I molecules per cell. (**C**) Statistical analysis of MHC-I positive cells. One-way ANOVA analysis of data, * = $P < 0.05$, ** = $P < 0.01$. Bars = Standard deviations.

lower concentration (~22 particles are observed in this section, as compared with > 150 particles in the trypomastigote kinetoplast section observed). Only one particle is detected in the kinetoplast section shown.

In infected cells, at 2 h PI (Figure 7A), GPs were observed in the parasitophorous vacuole, almost exclusively in the kinetoplast of the parasite. In the host cell, some GPs were observed in nuclear heterochromatin. At 4 h PI (Figure 7B), GPs were observed in the parasitophorous vacuole. Though there is a high-density label in the kinetoplast, some GPs are detected on the parasite nucleus and cytoplasm. In the host cell, some particles are observed in the nucleus and a few in the cytoplasm. At 6 h PI (Figure 7C), two parasites were observed inside parasitophorous vacuoles. In both cases, a high GP concentration is detected in their kinetoplasts. Much lower GP concentration is detected in the parasite nucleus and cytoplasm. No GPs were observed in a 6 h PI sample incubated with an anti-HuCD45 mouse IgG1 (isotype negative control, Figure 7D), or in a free trypomastigotes sample incubated with just the secondary antibody (Figure 7E).

The improvement in resolution, with the use of a larger GP size, and improvement in specificity with the use of a monoclonal antibody, allowed a simple manual quantification of the molecules detected in a different stage of the parasite. A representative set of results corresponding to epimastigotes, trypomastigotes, and trypomastigotes inside infected cells, is shown in Figure 8. More TcCRT molecules are detected in trypomastigote kinetoplast when the parasite is *inside* the host cell (Figure 8A and D) compared with free trypomastigotes (Figure 8B) or free epimastigotes (Figure 8C).

DISCUSSION

Previous reports showed the presence of TcCRT in the ER, as expected, but also in the Golgi, cytostome, in vesicles near the flagellum pocket, in the cytosol, and in the nucleus and kinetoplast in free trypomastigotes and epimastigotes. This evidence suggests a possible secretion pathway for

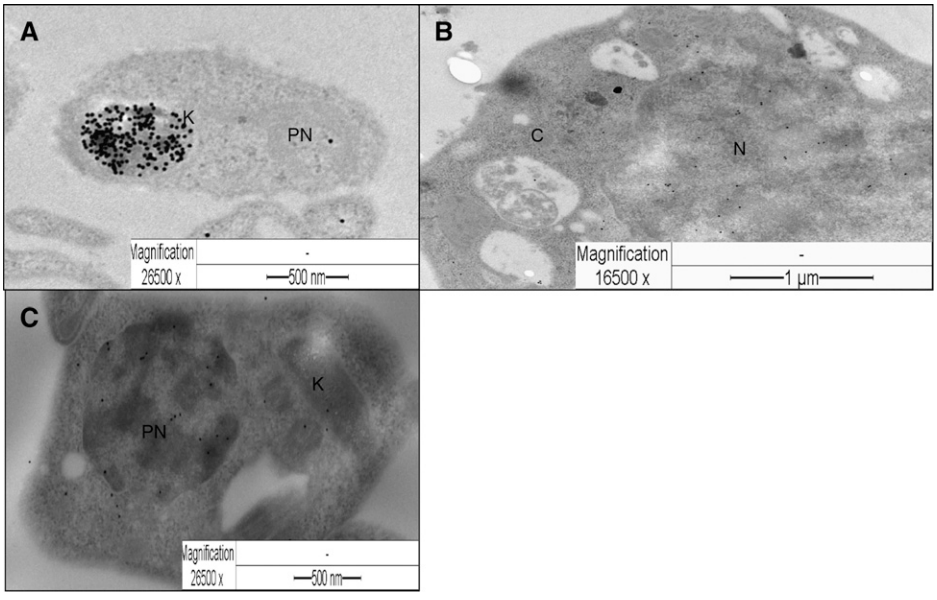

FIGURE 6. A MoAb E2G7 anti-TcCRT detects TcCRT in free parasites in transmission electron microscopy (TEM). Electron microphotographs of non-infected cells and free parasites are shown. Gold particles are observed in (**A**) a free trypomastigote, mainly in an oblique section of the kinetoplast (K); (**B**) a non-infected murine macrophage, mainly in nucleus as a background label; (**C**) a free epimastigote, mainly in the nucleus. A longitudinal section of an almost empty kinetoplast section was also presented. In host cell: N = nucleus; C = cytoplasm. In parasites: PN = parasite nucleus; K = kinetoplast. All samples were incubated with E2G7 anti-TcCRT monoclonal antibody, 1/100 v/v, followed by the corresponding gold-labeled secondary antibody, 1/20 v/v.

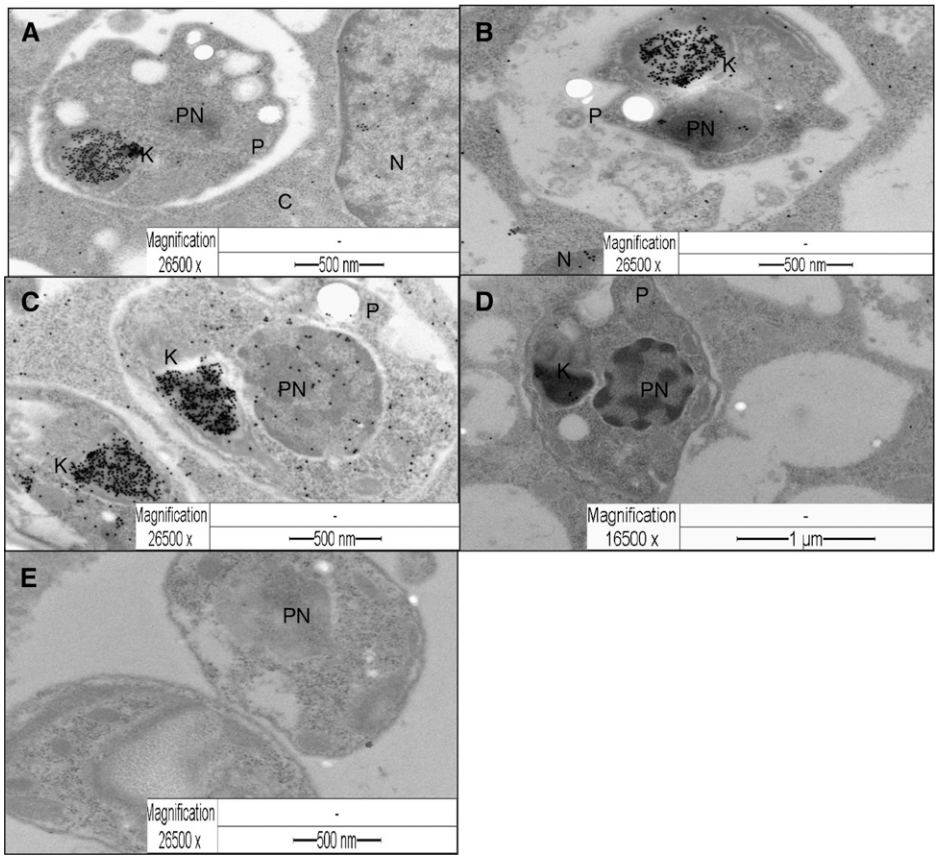

FIGURE 7. TcCRT is mainly found in the parasite kinetoplast inside infected cells. Electron microphotographs of infected cells are shown. Gold particles are observed at (**A**) 2 h PI, mainly in the parasite kinetoplast; (**B**) 4 h PI, mainly in the parasite kinetoplast, fewer in the parasite nucleus; (**C**) 6 h PI, in two intravacuolar parasites, mainly in the kinetoplast, but also in the parasite nucleus and cytoplasm. In negative control samples a (**D**) 6h PI and (**E**) free trypomastigotes, no gold particles were observed. In host cell: N = nucleus; C = cytoplasm. In parasites: P = parasite; PN = parasite nucleus; K = kinetoplast. Samples were incubated with: (**A**–**C**) E2G7 anti-TcCRT monoclonal antibody, 1/100 v/v; (**D**) anti-HuCD45, mouse IgG1 1/100 v/v, isotype negative control; (**E**) anti-mouse IgG conjugated to colloidal gold (18 nm), 1/20 v/v.

TcCRT.[9] More recently, this evidence is supported by other studies where two populations of vesicles, secreted by the parasite to the extracellular milieu, were analyzed and their protein cargo characterized. The TcCRT is among the 367 proteins identified.[29] The analyses of the vesicle cargo and localization of TcCRT were performed in free trypomastigotes and epimastigotes. No studies were performed on infected cells. This work provides new evidence regarding the localization of TcCRT on parasites *inside* the host cell.

As the different conditions required for immunocytochemistry do not allow a proper fixation of lipids and preservation of structures, Figure 1 shows a topographic control of each condition, in which organelles are clearly distinguished. In non-infected RAW 264.7 cells, we observed ribosomes (Figure 1A), with their expected 30 nm in diameter, thus serving as indicators of adequate resolution. Thus, 10 and 18 nm GPs, being more electron-dense than ribosomes, should be adequately resolved. Interestingly, at 4 h PI (Figure 1C), the host cell is extensively vacuolated. This might be caused by the infection process at this time gate.

Using a polyclonal anti-rTcCRT serum, we observed more GPs in infected cells (Figure 4). However, with polyclonal antibodies, some cross-reactive background is also present in non-infected cells (Figure 2A) (to compare the electron density of GPs and ribosomes, Figures 2A and 1A should be compared). Considering that CRT is highly conserved, it is likely that a rabbit antiserum generated against the parasite molecule will recognize the host-cell molecule, through those epitopes common to TcCRT and MmCRT. This cross-reactivity was minimized through a titration process (Supplemental Figure 1). In free epimastigotes (Figure 2B), TcCRT was observed mostly in the nucleus, as described.[9] In free trypomastigotes (Figure 2C), gold-particles were detected on the flagellum emergence zone and kinetoplast. It could be speculated that a "flow" of TcCRT from the kinetoplast toward the flagellum emergence zone occurs, because a decreasing gradient of GPs was observed between the kinetoplast and the extreme of the parasite (Figure 2C). Some GPs were observed in vesicle-like structures. Previous reports show that TcCRT is part of the protein cargo in vesicles secreted by the parasite.[29] Similarly, we have detected CRT *in situ inside* the vesicles, but *outside* the trypomastigote. This observation may complement the previous work, supporting a secretion pathway for TcCRT.[9] However, the possibility that the circular vesicle-type structure observed outside the parasite, where calreticulin was detected, may come from the host VERO cell, cannot be ruled out, because these parasites were harvested from the supernatant of these infected cells. Nonetheless, its attachment to the parasite plasma membrane supports its parasite origin.

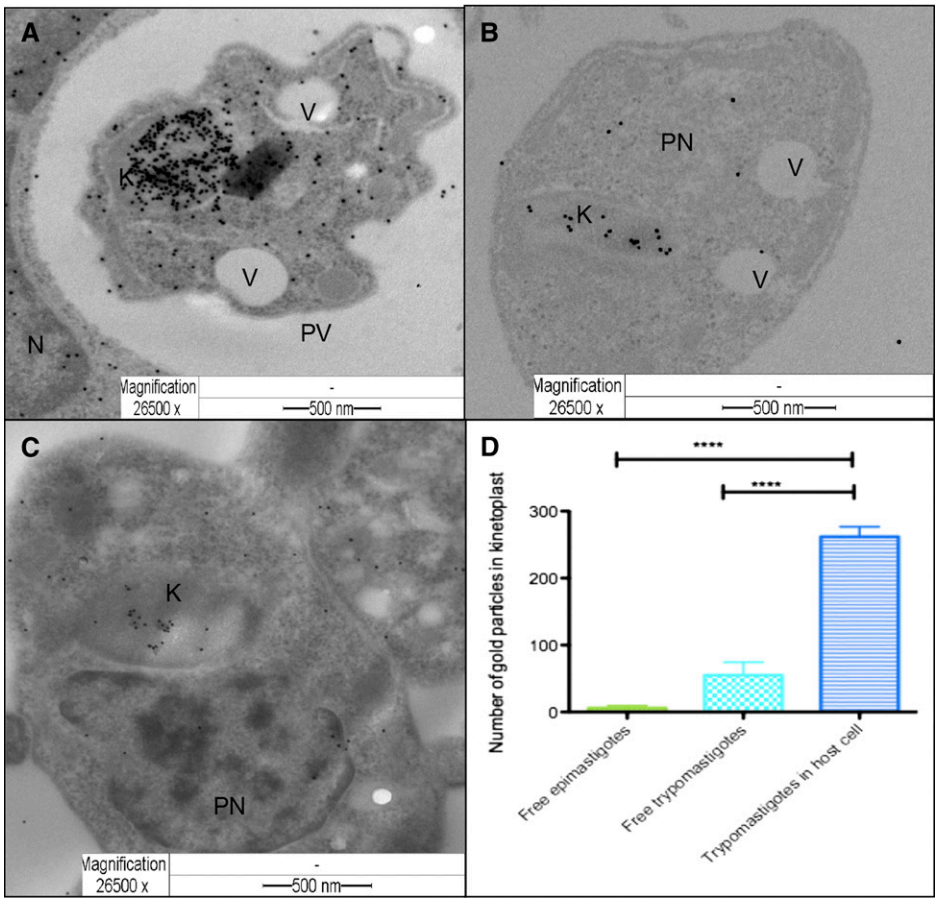

FIGURE 8. TcCRT presence is higher in the parasite kinetoplast of infected cells, as compared with free trypomastigotes or epimastigotes. Electron microphotographs of infecting and free parasites are shown. Gold particles are detected in (**A**) A 6 h PI sample, mainly in the trypomastigote kinetoplast (K), but also detected in the parasite nucleus and host cell cytoplasm. (**B**) A free trypomastigote, almost exclusively in the kinetoplast (K). (**C**) A free epimastigote, in nucleus and kinetoplast. (**D**) Number of gold particles detected in kinetoplast sections, is higher in infecting parasites ($N = 6$ for free trypomastigotes and epimastigotes, $N = 5$ for trypomastigotes in the host cell). (**A**–**C**) MoAb E2G7 anti-TcCRT 1/100 v/v; (**D**) One-way ANOVA analysis, **** = $P < 0.0001$. In host cell: N = nucleus. In parasites: PV = parasitophorous vacuole; PN = parasite nucleus; V = Vacuoles; K = kinetoplast.

At 4 h PI, other circular structures, with a positive gold label, were observed in close proximity to the parasitophorous vacuole (data not shown), outside the host cell. The vesicle-like structures seen in Figures 2C and 3A are 35–38 nm in diameter, consistent with those previously described for metacyclic trypomastigotes.[29]

In infected cells (Figure 3A–C), GPs were observed in different parasite and host cell organelles. In the parasite, the kinetoplast and the nucleus, the organelles with the highest DNA concentration, presented the maximum density label. At 2 (Figure 3A) and 6 h PI (Figure 3C), when the parasite is observed *inside* the parasitophorous vacuole, vesicle-like structures are detected with positive gold label *inside* the parasite, in the parasitophorous vacuole (*outside* the parasite), and, in the host cell cytoplasm. These structures were previously observed inside metacyclic trypomastigotes.[9] In the host cell, some particles are observed in the cytoplasm and nucleus. As a result of the sensitivity of the technique used, it is not possible to discriminate, at this point, the origin (parasite or host cell) of the protein that is detected by the anti-rTcCRT polyclonal serum in the host cell. At 4 h PI (Figure 3B), a parasite is observed outside the host cell, before being phagocytosed. As previously reported, high-density label was observed in the parasite nucleus and kinetoplast. In the host cell, GPs were observed both in nuclear heterochromatin and cytoplasm, facts again consistent with previous results (Figure 3A).[9] No extensive vacuolization could be observed in the host-cell, suggesting that this phenomenon is a response to parasite internalization. None of the controls performed at 6 h PI, in the absence of primary antibody (Figure 3D) or with preimmune serum (Figure 3E), showed GPs.

The fact that at 2 h PI, there are more CRT molecules in the nucleus and cytoplasm (Figure 4A), reaching a maximum at 4 h PI (Figure 4B), in all organelles analyzed, could be explained as follows: i) TcCRT is externalized by the parasite reaching the host cell cytoplasm and the nucleus at 4 h PI. Interestingly, *T. cruzi* infection modulates negatively the over-expression of MHC-I molecules on the membrane when induced with lipopolysaccharide (LPS),[30] whereas in other studies it showed no effect[31] and, ii) Alternatively or concomitantly, a MmCRT peak observed at 4 h PI, possibly overexpressed during infection, is detected by anti-rTcCRT antibodies present in the polyclonal serum, that cross-react with MmCRT.

At 6 h PI, there are more CRT molecules in infected cells compared with the non-infected counterpart only in

the nucleus (Figure 4C). In cytoplasm, no significant differences were obtained. In the parasitophorous vacuole, at 6 h PI, there is a decrease in the number of GPs detected, compared with 2 or 4 h PI, which could indicate mobilization of TcCRT toward the host cell cytoplasm, because these putative microvesicles were observed here in close proximity to the parasitophorous vacuole.

The CRT is a key molecule in the MHC-I folding process. Less MHC-I positive cells were detected at 2 and 4 h PI (Figure 5A and C). When the percentage of maximum fluorescence was analyzed, no differences between experimental time gates were found (Figure 5B). Possible explanations to this result include: i) Because the number of MHC-I positive cells, which were selected in the flow cytometry analysis, decreased substantially in the infected cells, at 2 and 4 h, PI, the possibility exists that the infective challenge killed a proportion of these cells. Furthermore, extensive vacuolization is observed at 4 h PI, together with CRT externalization in apoptotic cells, as a damage-associated molecular pattern (DAMP)[32–34]; ii) Alternatively or concomitantly, TcCRT accesses to the host cell cytoplasm at 2 h PI, reaching its peak at 4 h PI. Whether TcCRT accesses to host cell ER, and there competes with MmCRT in promoting the correct MHC-I molecule folding, is unknown. In agreement with this possibility, the peak of CRT detection is at 4 h PI, the same time gate where less MHC-I positive cells are detected. Moreover, the vesicle-like structures observed with the anti-rTcCRT polyclonal serum (Figure 3A and C) supports the access of TcCRT into the host cell cytoplasm. Perhaps, the parasite uses its CRT not only to access the host cell,[5] but also to evade antigen presentation.[30] However, this secretion might induce translocation of the host cell CRT that can be recognized as DAMP by innate immune mechanisms, with subsequent elimination of the infected cell during the first hours post-infection.

A monoclonal antibody anti-TcCRT (E2G7), did not recognize antigens in a whole cell extract of RAW 264.7 cells in IWB and ELISA (data not shown). Interestingly, E2G7 apparently discriminates TcCRT according to its functional state. For example, although it does not recognize externalized native TcCRT in flow cytometry, most likely because the epitope is not accessible to the antibody (Ferreira and others, unpublished data), it does recognize the molecule in different compartments of the free and infecting parasites.

In free trypomastigotes (Figure 6A), GPs are detected almost exclusively in the kinetoplast and very seldom in other organelles. Whether the epitope recognized by E2G7 is correctly exposed mainly in the kinetoplast, remains to be determined. In non-infected RAW cells (Figure 6B), some particles are detected by E2G7 in the nucleus and cytoplasm, as a background label. Even though previous tests with E2G7 in RAW 264.7 whole cell extracts, showed no cross-reactivity (data not shown), it is possible that the higher sensitivity of TEM detects it. In epimastigotes (Figure 6C) label is observed mainly in the nucleus, and few particles are detected in the kinetoplast.

In infected-cells (Figure 7A–C) the common pattern is a significant label in the kinetoplast, in all conditions analyzed (2, 4, and 6 h PI). Only a few molecules can be observed in the parasite nucleus and in the host cell cytoplasm and nucleus. At this point, we cannot define whether these few particles correspond to parasite or host CRT.

Remarkably, the kinetoplast is the organelle where GPs are detected in a high concentration with the monoclonal and polyclonal anti-rTcCRT antibodies, in all samples analyzed. According to previous reports, using polyclonal anti-rTcCRT antibodies, the kinetoplast is the organelle that presents more GPs/μm^2 in *free* trypomastigotes.[9]

Because different sections of the parasite kinetoplast were analyzed, as a result of statistical possibilities, oblique and transverse sections were observed more often (Supplemental Figure 3).

The kinetoplast is near the flagellum emergence zone (Figure 2C) where condensation of vesicles has been reported in the flagellum pocket.[35] One possible explanation for the high-density label in the kinetoplast is that this organelle acts as a reservoir of TcCRT before it can access the flagellum pocket zone during the externalization process. Another possible role for CRT is gene expression/transcription regulation. Thus, CRT binds nuclear glucocorticoid receptors[36,37] that regulate gene expression/repression. The possibility that CRT may regulate transcription in the kinetoplast cannot be discarded. A third likely possibility to explain TcCRT presence in the kinetoplast would be the Ca^{+2} signaling regulation and storage. In mammals, mitochondria and ER interaction depends on Ca^{+2} signaling.[38] Moreover, impaired functions in mitochondria have been described when a truncated form of CRT is expressed.[39] No GPs were observed in infected cells 6 h PI incubated with an anti-HuCD45 monoclonal antibody (Figure 7D) or in trypomastigotes incubated with just the secondary probe (Figure 7E).

Before incubation with the primary antibody (monoclonal or polyclonal) and to prevent non-specific binding of GPs, the nickel grids were treated with a blocking buffer (see Methods). This procedure was effective because the negative

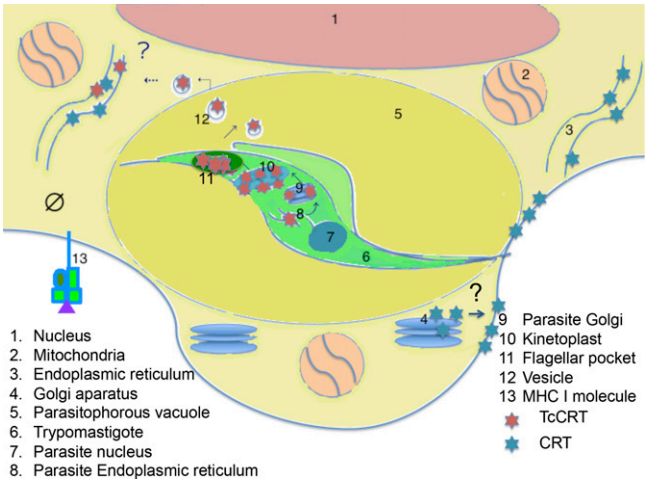

FIGURE 9. Proposed model of possible TcCRT externalization *inside* host cells. Possible route followed by TcCRT, which includes several organelles like parasite's ER, Golgi and kinetoplast, and possible effects on the host cell CRT. From the parasite ER, TcCRT suffers post-translational modifications in the Golgi apparatus. Once modified in Golgi, TcCRT accumulates in the kinetoplast, before it accesses to the flagellum pocket, from which it is secreted to the parasite exterior, possibly through microvesicles. Once in the host cell cytoplasm, it could have functional implications such as down-regulation of MHC-I molecules, or promoting MmCRT overexpression.

controls (pre-immune serum, isotype control, and incubation with just the secondary antibody) showed no GPs.

The use of a monoclonal antibody, the increase of GP size, and the change of microscope, form a Zeiss EM-109 to a Phillip-TECNAI 12, all contributed to an important increase in sensitivity and resolution. Our results are comparable to those obtained in other models, with an acrylic resin at low temperature, used in the inclusion process.[40]

The number of GPs in the kinetoplasts of infecting trypomastigotes (those found inside the parasitophorous vacuoles) was at least five times higher than those detected in free epimastigotes and trypomastigotes (Figure 8). The resolution and sensitivity of our procedure was such that a simple direct counting of GPs was possible, with reproducible results. The possibility that infecting parasites might upregulate the expression of TcCRT once they are *inside* the host cell cannot be discarded. Indeed, TcCRT mRNA increases in the first 24 hrs PI,[5] in agreement with our results.

Whether the differences detected in TcCRT distribution among parasite organelles are causally related with infectivity, is a subject of current investigations in our laboratories.

In Figure 9, we speculate on possible TcCRT pathways from the parasite ER to the parasite exterior, when located *inside* the host cell. A peptide signal allows TcCRT to exit the parasite's ER, followed by access to the parasite Golgi where it sustains post-translational modifications, previous to its externalization. It then converges in the parasite kinetoplast, with unknown functions. This may be used as a stopover before its final access to the flagellum emergence zone. Outside the parasite, TcCRT may cross the parasitophorous vacuole and access the host cell cytoplasm. Once there, possibly through mechanisms similar to those used by virus or bacterial toxins,[41,42] it may access the host cell ER, where a competition with the host cell CRT is conceivable.

CONCLUSIONS

This is the first study that shows a chaperone parasite molecule, such as CRT, *inside* host cells during the infective process. The TcCRT undergoes precise variations in its topographical locations, both in the parasite and host cell. Thus, on the one hand, TcCRT accumulates in the infective trypomastigote kinetoplast, but not in the organelle present in non-infective epimastigotes. On the other hand, a polyclonal antibody anti-TcCRT detects an increase in the chaperone (possibly of parasite origin), in the infected host cell (nucleus and cytoplasm). Moreover, MHC-I positive host cells decrease at the first hours post-infection. Future studies will aim at deciphering how these variations functionally correlate with infective capacity.

Received August 7, 2014. Accepted for publication December 29, 2014.

Published online March 9, 2015.

Note: Supplemental figures appear at www.ajtmh.org.

Acknowledgments: We thank Dr. Karina Pino-Lagos for her support in the analysis of flow cytometry data, and Carlos Rosas for his support in image editing.

Financial support: This work was supported by FONDECYT grant 1130099 (AF) and Associative Research ACT-112 (AF, NG), FONDECYT grant 1130113 (NG), and also CONICYT fellowships: For Doctoral Studies in Chile (21080219) and Doctoral Thesis Support (AT 24100233) (AG).

Authors' addresses: Andrea González, Caroline Valck, and Arturo Ferreira, University of Chile, Program of Immunology, Institute of Biomedical Sciences, Faculty of Medicine, Santiago, Chile, E-mails: angozu@ciq.uchile.cl, cvalck@gmail.com, and aferreir@med.uchile.cl. Gittith Sánchez, University of Chile, Program of Human Genetics, Institute of Biomedical Sciences, Faculty of Medicine, Santiago, Chile, E-mail: gsanchez@med.uchile.cl. Steffen Härtel and Jorge Mansilla, University of Chile, Biomedical Neuroscience Institute, Institute of Biomedical Sciences, Faculty of Medicine, Santiago, Chile, E-mails: shartel@med.uchile.cl and jorgemansillas@gmail.com. Galia Ramírez, University of Chile, Department of Preventing Animal Medicine, Faculty of Veterinarian Medicine, Santiago, Chile, E-mail: galiaramirez@gmail.com. María Soledad Fernández and José L. Arias, University of Chile, Department of Animal Biological Sciences, Faculty of Veterinarian Medicine, Santiago, Chile, E-mails: sofernan@uchile.cl and jarias@uchile.cl. Norbel Galanti, University of Chile, Program of Cellular and Molecular Biology, Institute of Biomedical Sciences, Faculty of Medicine, Santiago, Chile, E-mail: ngalanti@med.uchile.cl.

REFERENCES

1. Clayton J, 2010. Chagas disease 101. *Nature 465:* S4–S5.
2. Clayton J, 2010. Chagas disease: pushing through the pipeline. *Nature 465:* S12–S15.
3. Coura JR, Vinas PA, 2010. Chagas disease: a new worldwide challenge. *Nature 465:* S6–S7.
4. Tyler KM, Engman DM, 2001. The life cycle of *Trypanosoma cruzi* revisited. *Int J Parasitol 31:* 472–481.
5. Ramirez G, Valck C, Molina MC, Ribeiro CH, Lopez N, Sanchez G, Ferreira VP, Billetta R, Aguilar L, Maldonado I, Cattan P, Schwaeble W, Ferreira A, 2011. *Trypanosoma cruzi* calreticulin: a novel virulence factor that binds complement C1 on the parasite surface and promotes infectivity. *Immunobiology 216:* 265–273.
6. Ferreira V, Molina MC, Valck C, Rojas A, Aguilar L, Ramirez G, Schwaeble W, Ferreira A, 2004. Role of calreticulin from parasites in its interaction with vertebrate hosts. *Mol Immunol 40:* 1279–1291.
7. Michalak M, Corbett EF, Mesaeli N, Nakamura K, Opas M, 1999. Calreticulin: one protein, one gene, many functions. *Biochem J 344:* 281–292.
8. Sonnichsen B, Fullekrug J, Nguyen Van P, Diekmann W, Robinson DG, Mieskes G, 1994. Retention and retrieval: both mechanisms cooperate to maintain calreticulin in the endoplasmic reticulum. *J Cell Sci 107:* 2705–2717.
9. Souto-Padron T, Labriola CA, de Souza W, 2004. Immunocytochemical localization of calreticulin in *Trypanosoma cruzi*. *Histochem Cell Biol 122:* 563–569.
10. Mesaeli N, Nakamura K, Zvaritch E, Dickie P, Dziak E, Krause KH, Opas M, MacLennan DH, Michalak M, 1999. Calreticulin is essential for cardiac development. *J Cell Biol 144:* 857–868.
11. Ferreira V, Valck C, Sanchez G, Gingras A, Tzima S, Molina MC, Sim R, Schwaeble W, Ferreira A, 2004. The classical activation pathway of the human complement system is specifically inhibited by calreticulin from *Trypanosoma cruzi*. *J Immunol 172:* 3042–3050.
12. Valck C, Ramirez G, Lopez N, Ribeiro CH, Maldonado I, Sanchez G, Ferreira VP, Schwaeble W, Ferreira A, 2010. Molecular mechanisms involved in the inactivation of the first component of human complement by *Trypanosoma cruzi* calreticulin. *Mol Immunol 47:* 1516–1521.
13. Ramirez G, Valck C, Ferreira VP, Lopez N, Ferreira A, 2012. Extracellular *Trypanosoma cruzi* calreticulin in the host-parasite interplay. *Trends Parasitol 27:* 115–122.
14. Sosoniuk E, Vallejos G, Kenawy H, Gaboriaud C, Thielens N, Fujita T, Schwaeble W, Ferreira A, Valck C, 2014. *Trypanosoma cruzi* calreticulin inhibits the complement lectin pathway activation by direct interaction with L-ficolin. *Mol Immunol 60:* 80–85.
15. Lopez NC, Valck C, Ramirez G, Rodriguez M, Ribeiro C, Orellana J, Maldonado I, Albini A, Anacona D, Lemus D, Aguilar L, Schwaeble W, Ferreira A, 2010. Antiangiogenic and antitumor effects of *Trypanosoma cruzi* calreticulin. *PLoS Negl Trop Dis 4:* e730.

16. Molina MC, Ferreira V, Valck C, Aguilar L, Orellana J, Rojas A, Ramirez G, Billetta R, Schwaeble W, Lemus D, Ferreira A, 2005. An *in vivo* role for *Trypanosoma cruzi* calreticulin in antiangiogenesis. *Mol Biochem Parasitol 140:* 133–140.
17. Ferreira V, Molina MC, Schwaeble W, Lemus D, Ferreira A, 2005. Does *Trypanosoma cruzi* calreticulin modulate the complement system and angiogenesis? *Trends Parasitol 21:* 169–174.
18. Sanchez Valdez FJ, Perez Brandan C, Zago MP, Labriola C, Ferreira A, Basombrio MA, 2013. *Trypanosoma cruzi* carrying a monoallelic deletion of the calreticulin (TcCRT) gene are susceptible to complement mediated killing and defective in their metacyclogenesis. *Mol Immunol 53:* 198–205.
19. Sanchez-Valdez FJ, Perez Brandan C, Ramirez G, Uncos AD, Zago MP, Cimino RO, Cardozo RM, Marco JD, Ferreira A, Basombrio MA, 2014. A monoallelic deletion of the TcCRT gene increases the attenuation of a cultured *Trypanosoma cruzi* strain, protecting against an *in vivo* virulent challenge. *PLoS Negl Trop Dis 8:* e2696.
20. Aguillon JC, Ferreira L, Perez C, Colombo A, Molina MC, Wallace A, Solari A, Carvallo P, Galindo M, Galanti N, Orn A, Billetta R, Ferreira A, 2000. Tc45, a dimorphic *Trypanosoma cruzi* immunogen with variable chromosomal localization, is calreticulin. *Am J Trop Med Hyg 63:* 306–312.
21. Aguilar L, Ramirez G, Valck C, Molina MC, Rojas A, Schwaeble W, Ferreira V, Ferreira A, 2005. F(ab′)2 antibody fragments against *Trypanosoma cruzi* calreticulin inhibit its interaction with the first component of human complement. *Biol Res 38:* 187–195.
22. Aguillon JC, Harris R, Molina MC, Colombo A, Cortes C, Hermosilla T, Carreno P, Orn A, Ferreira A, 1997. Recognition of an immunogenetically selected *Trypanosoma cruzi* antigen by seropositive chagasic human sera. *Acta Trop 63:* 159–166.
23. Kohler G, Milstein C, 1975. Continuous cultures of fused cells secreting antibody of predefined specificity. *Nature 256:* 495–497.
24. Yasumura YK, Kawakita M, 1963. The research for the SV40 by means of tissue culture technique. *Nippon Rinsho 21:* 1201–1219.
25. Paulsson K, Wang P, 2003. Chaperones and folding of MHC class I molecules in the endoplasmic reticulum. *Biochim Biophys Acta 1641:* 1–12.
26. Mancino L, Rizvi SM, Lapinski PE, Raghavan M, 2002. Calreticulin recognizes misfolded HLA-A2 heavy chains. *Proc Natl Acad Sci USA 99:* 5931–5936.
27. Saito Y, Ihara Y, Leach MR, Cohen-Doyle MF, Williams DB, 1999. Calreticulin functions *in vitro* as a molecular chaperone for both glycosylated and non-glycosylated proteins. *EMBO J 18:* 6718–6729.
28. Wada I, Imai S, Kai M, Sakane F, Kanoh H, 1995. Chaperone function of calreticulin when expressed in the endoplasmic reticulum as the membrane-anchored and soluble forms. *J Biol Chem 270:* 20298–20304.
29. Bayer-Santos E, Aguilar-Bonavides C, Rodrigues SP, Cordero EM, Marques AF, Varela-Ramirez A, Choi H, Yoshida N, da Silveira JF, Almeida IC, 2012. Proteomic analysis of *Trypanosoma cruzi* secretome: characterization of two populations of extracellular vesicles and soluble proteins. *J Proteome Res 12:* 883–897.
30. Van Overtvelt L, Andrieu M, Verhasselt V, Connan F, Choppin J, Vercruysse V, Goldman M, Hosmalin A, Vray B, 2002. *Trypanosoma cruzi* down-regulates lipopolysaccharide-induced MHC class I on human dendritic cells and impairs antigen presentation to specific CD8(+) T lymphocytes. *Int Immunol 14:* 1135–1144.
31. Buckner FS, Wipke BT, Van Voorhis WC, 1997. *Trypanosoma cruzi* infection does not impair major histocompatibility complex class I presentation of antigen to cytotoxic T lymphocytes. *Eur J Immunol 27:* 2541–2548.
32. Gardai SJ, McPhillips KA, Frasch SC, Janssen WJ, Starefeldt A, Murphy-Ullrich JE, Bratton DL, Oldenborg PA, Michalak M, Henson PM, 2005. Cell-surface calreticulin initiates clearance of viable or apoptotic cells through trans-activation of LRP on the phagocyte. *Cell 123:* 321–334.
33. Tarr JM, Young PJ, Morse R, Shaw DJ, Haigh R, Petrov PG, Johnson SJ, Winyard PG, Eggleton P, 2010. A mechanism of release of calreticulin from cells during apoptosis. *J Mol Biol 401:* 799–812.
34. Kuraishi T, Manaka J, Kono M, Ishii H, Yamamoto N, Koizumi K, Shiratsuchi A, Lee BL, Higashida H, Nakanishi Y, 2007. Identification of calreticulin as a marker for phagocytosis of apoptotic cells in *Drosophila*. *Exp Cell Res 313:* 500–510.
35. Landfear SM, Ignatushchenko M, 2001. The flagellum and flagellar pocket of trypanosomatids. *Mol Biochem Parasitol 115:* 1–17.
36. Dedhar S, Rennie PS, Shago M, Hagesteijn CY, Yang H, Filmus J, Hawley RG, Bruchovsky N, Cheng H, Matusik RJ, 1994. Inhibition of nuclear hormone receptor activity by calreticulin. *Nature 367:* 480–483.
37. Burns K, Duggan B, Atkinson EA, Famulski KS, Nemer M, Bleackley RC, Michalak M, 1994. Modulation of gene expression by calreticulin binding to the glucocorticoid receptor. *Nature 367:* 476–480.
38. Simpson L, 1987. The mitochondrial genome of kinetoplastid protozoa: genomic organization, transcription, replication, and evolution. *Annu Rev Microbiol 41:* 363–382.
39. Arnaudeau S, Frieden M, Nakamura K, Castelbou C, Michalak M, Demaurex N, 2002. Calreticulin differentially modulates calcium uptake and release in the endoplasmic reticulum and mitochondria. *J Biol Chem 277:* 46696–46705.
40. Jaime Renau Piqueras LM, 1998. *Manual de Técnicas de Microscopía Electrónica (MET) Aplicaciones Biológicas*.
41. Roder G, Geironson L, Bressendorff I, Paulsson K, 2008. Viral proteins interfering with antigen presentation target the major histocompatibility complex class I peptide-loading complex. *J Virol 82:* 8246–8252.
42. Spooner RA, Smith DC, Easton AJ, Roberts LM, Lord JM, 2006. Retrograde transport pathways utilised by viruses and protein toxins. *Virol J 3:* 26.